CHEMISTRY
A European Journal

A Journal of
ChemPubSoc Europe

Accepted Article

Title: Effect of the metal within regioisomeric paddle-wheel-type metal-organic frameworks

Authors: Hyeonbin Ha, Youngik Kim, Dopil Kim, Jihyun Lee, Yoodae Song, Suyeon Kim, Myung Hwan Park, Youngjo Kim, Hyungjun Kim, Minyoung Yoon, and Min Kim

To be cited as: *Chem. Eur. J.* 10.1002/chem.201903210

Link to VoR: http://dx.doi.org/10.1002/chem.201903210

Supported by
ACES

WILEY-VCH

10.1002/chem.201903210

WILEY-VCH

Effect of the metal within regioisomeric paddle-wheel-type metal-organic frameworks

Hyeonbin Ha,[a]† Youngik Kim, [a]† Dopil Kim, [a]† Jihyun Lee,[b] Yoodae Song,[b] Suyeon Kim,[a] Myung Hwan Park,[c] Youngjo Kim,[a] Hyungjun Kim,*[d] Minyoung Yoon,* [b,e] and Min Kim*[a]

Abstract: The effect of metal on the degree of flexibility upon evacuation of metal-organic frameworks (MOFs) has been revealed with positional control of the organic functionalities. While Co-, Cu-, and Zn-based DMOFs with *ortho*-ligands (2,3-NH_2Cl) have frameworks that are inflexible upon evacuation, MOFs with *para*-ligands (2,5-NH_2Cl) showed different N_2 uptake amounts after evacuation by metal exchange. Since the structural analysis were not fully sufficiently different to explain the drastic changes in N_2 adsorption after evacuation, quantum chemical simulation was explored. A new index (η) was defined to quantify the regularity around the metal based on differences in the oxygen-metal-oxygen angles. Within 2,5-NH_2Cl, the η value becomes larger as the metal are varied from Co to Zn. A large η value means that the structures around the metal center are less ordered. These results can be used to explain flexibility changes upon evacuation by altering the metal cation in this regioisomeric system.

Introduction

Metal-organic frameworks (MOFs) are three-dimensional, porous, organic-inorganic hybrid materials that consist of inorganic nodes and multivalent organic struts. The size of the pore and pore environment can be tuned by varying the combination of metal cluster (or ion) and functional groups on the organic linker. These hybrid materials have been intensely studied for a variety of applications, such as gas storage, molecular separation, and catalysis, due to their unique porous characteristics with a variety of functional groups.[1–4] Since MOFs are constructed by infinite coordination bonds between metal ions and chelating ligands, they are also called porous coordination polymers (PCPs). These coordination bonds could give MOFs some structural flexibility, and the framework and/or the pore size could be changed by this flexible nature. External stimuli, such as the presence of guest molecules, molecular adsorption, and solvent evacuation, could allow structural changes in flexible MOF systems.[5,6]

The flexible structures of MOFs are mainly dependent on the type of secondary building unit (SBU) and coordinated ligands present. For example, zinc-based IRMOFs (isoreticular MOFs), which consists of Zn_4O SBU and benzene-1,4-dicarboxylate (BDC) ligands, displayed a very rigid structure. However, zinc-paddle wheel-type DMOFs (DABCO MOF, DABCO = 1,4-diazabicylco[2.2.2]octane), which consist of Zn_2 paddle-wheel SBU, BDC, and DABCO ligands, showed a flexible structure upon external stimuli.[5,6] In addition, aluminum-based MOFs also showed flexibility differences based on wine-rack type structures.[7,8] While MIL-53(Al)-NH_2 (MIL = Materials from Institute of Lavoisier) showed flexible structures depending on external stimuli, and another aluminum-based MOF, MIL-101(Al)-NH_2, is known for its rigidity.[5]

Although the flexibility of MOFs naturally arises from the type of coordination bonds between the metal nodes and strut, the functional groups (i.e., chemical tag) on the organic linkers also have significant effects on the flexibility changes of MOFs. Fischer and coworkers studied the functionalization of flexible MOFs in great detail. BDC ligands with a series of different functionalities/alkyl chain lengths were prepared and used to construct to DMOFs. The flexibility of the DMOFs was controlled by the alkyl chain length and the degree of saturation in the chemical tags.[9,10] Recently, Cohen's group and our group have revealed that not only direct interframework interactions between two linkers but also the electronic environment of the ligands are significantly correlated with the flexibility of the MOFs.[11–13] We prepared a series of bifunctionalized BDC ligands with two chemical handles along with regioisomeric differences. All symmetrical and unsymmetrical combinations of NH_2, NO_2, OMe, and Cl functionalities at the *ortho*- and *para*-positions were synthesized and used to construct DMOFs. Among the 10 combinations, only diamino-functionalized BDCs could not successfully be incorporated into DMOFs due to their low thermal stability and solubility under solvothermal conditions.[13] Of the remaining 9 combinations, only *para*-substituted amino-halo, amino-methoxy, and dimethoxy-functionalized DMOFs (i.e., DMOF-2,5-NH_2X, DMOF-2,5-NH_2OMe, and DMOF-2,5-$(OMe)_2$)

[a] H. Ha, Y. Kim, D. Kim. S. Kim, Prof. Dr. Y. Kim, Prof. Dr. M. Kim
Department of Chemistry and BK21Plus Research Team
Chungbuk National University
1 Chungdae-ro, Seowon-gu, Cheongju, 28644, Republic of Korea
E-mail: minkim@chungbuk.ac.kr
[b] J. Lee, Y. Song, Prof. M. Yoon
Department of Nanochemistry
Gachon University
1342 Seongnamdae-ro, Sujeong-gu, Seongnam, 13120, Republic of Korea
E-mail: myyoon@gachon.ac.kr
[c] Prof. Dr. M. H. Park
Department of Chemistry Education
Chungbuk National University
1 Chungdae-ro, Seowon-gu, Cheongju, 28644, Republic of Korea
[d] Prof. Dr. H. Kim
Department of Chemistry
Incheon National University
119 Academy-ro, Yeonsu-gu, Incheon 22012, Republic of Korea
E-mail: kim.hyungjun@inu.ac.kr
[e] Prof. Dr. M. Yoon
Department of Chemistry
Kyungpook National University
80 Daehak-ro, buk-gu, Daegu, 41566, Republic of Korea
E-mail: myyoon@knu.ac.kr

Supporting information for this article is given via a link at the end of the document.

resulted in flexible frameworks upon evacuation. These three ligands have more electron-rich benzene rings relative to those in the other ligands (*e.g.*, NH_2-NO_2, NO_2-OMe, OMe-Cl, NO_2-Cl, NO_2-NO_2, and Cl-Cl) based on their Hammett constants.[12,13] Herein, we focused on the effect of the metal on the magnitude of the flexibility changes in the regioisomeric DMOF systems. Three DMOFs of cobalt, copper, and zinc with *ortho*- and *para*-NH_2-Cl-functionalities will be compared based on their gas adsorption differences after evacuation. There are several reports about the relationships between flexibility (as well as breathing behavior and gate-opening) and the metal cation on MOFs.[14–19] In particular, Kaskel and coworkers prepared a series of DUT-8 MOFs (DUT = Dresden University of Technology) with Ni, Cu, Co, and Zn and studied the magnitude of the changes in flexibility with different metal nodes. DUT-8 species are also DABCO-based pillared MOFs with a slightly tilted 2,6-naphthalenedicarboxylic acid). In their results, Ni and Co produces flexible and reversible frameworks, Zn-based DUT-8 formed flexible-irreversible frameworks, and Cu-based DUT-8 formed inflexible structures.[14] Very recently, Fischer's research team studied the effect of the metal on methoxyethoxy-functionalized DMOFs. Both the cobalt and nickel derivatives showed structural swelling and switching, and the copper-based MOFs and zinc-based MOFs showed only structural switching.[19] Both Kaskel's DUT-8 studies and Fischers's DMOF studies clearly indicate that the metal cation could impact the flexibility of DMOFs; thus, in this study, we want to focus the relationship between the regioisomer of the ligand and the flexibility of MOFs with a metal salt.

Results and Discussion

Synthesis of the Ligands and MOFs

Both BDC-2,3-NH_2Cl (**1**) and BDC-2,5-NH_2Cl (**2**) ligands were prepared by following reported procedures.[11] Regioisomeric mixtures of methyl esters **1** and **2** were synthesized by the chlorination of dimethyl-2-amino terephthalate (BDCE-NH_2), and esters **1** and **2** were separated by column chromatography. The hydrolysis of each ester with potassium hydroxide gave desired ligand **1** or **2** as the carboxylic acid (Scheme S1). Using these regioisomeric ligands, the syntheses of DMOFs with different metal salts were attempted. Zinc-based DMOFs was first reported by K. Kim *et al.* in 2003.[20] Walton and coworkers successfully prepared cobalt-, nickel-, copper-, and zinc-based DMOF-1 without organic functional groups and studied their stability to humidity.[21] Based on their synthetic conditions with different metal salts, we attempted to synthesize DMOF(Co), DMOF(Ni), DMOF(Cu), and DMOF(Zn) with two regioisomeric ligands, BDC-2,3-NH_2Cl and BDC-2,5-NH_2Cl. First, for zinc, both DMOF(Zn)-2,3-NH_2Cl and DMOF(Zn)-2,5-NH_2Cl were successfully obtained as colorless crystals, as reported (Scheme 1).[11] Second, in the case of cobalt, cobalt(II) nitrate was used as the metal source instead of $Zn(NO_3)_2$. The solvothermal syntheses of the DMOF(Co)s had to be performed in an autoclave. Both DMOF(Co)-2,3-NH_2Cl and DMOF(Co)-2,5-NH_2Cl were also successfully synthesized and were obtained as purple crystals (Scheme 1). However, the nickel-based DMOFs, DMOF(Ni)-2,3-NH_2Cl and DMOF(Ni)-2,5-NH_2Cl, were not obtained after a thorough screening of synthetic conditions. Since there is limited literature on functional group-containing Ni-MOFs from BDC-type ligands, we explored the synthesis of mono-functionalized DMOF(Ni) species rather than regioisomeric, bifunctional species. Interestingly, we could obtain DMOF(Ni)-1-Cl, but not DMOF(Ni)-1-NH_2, under solvothermal conditions (Figure S1, see the Supporting Information for details). To date, there are very limited reports about Ni(II)-based MOFs with NH_2-functionalized ligands.[22,23] We hypothesize that the coordination between nickel(II) and BDC-NH_2 prevents the formation of DMOFs under solvothermal conditions.

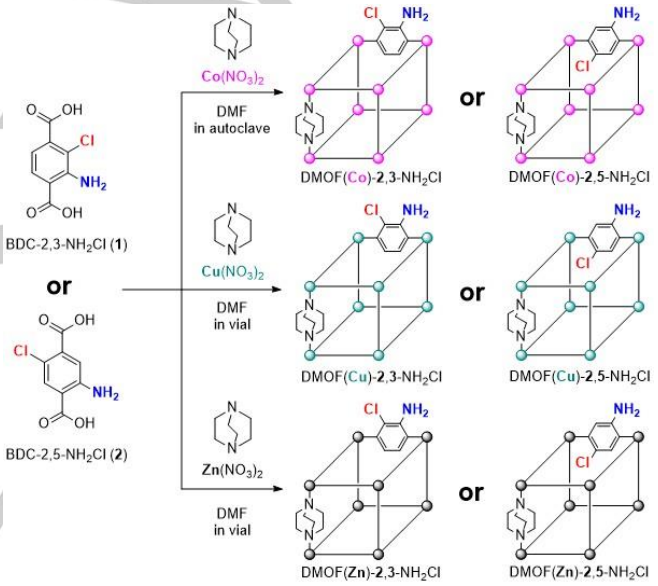

Scheme 1. Synthesis of regioisomeric DMOFs with different metal salts (colored circle = M_2 secondary building unit).

Finally, we studied the synthesis of copper-based DMOFs. Interestingly, both DMOF(Cu)-2,3-NH_2Cl and DMOF(Cu)-2,5-NH_2Cl were obtained as powdery microcrystals (Scheme 1). Although the morphology varied with the metal salt (Co, Cu, and Zn), the DMOF structures were perfectly constructed with the two regioisomeric ligands, as evidenced by power X-ray diffraction (PXRD, Figure 1). ^{1}H NMR measurements after acid digestion confirmed that each ligand was completely retained in the frameworks (Figure S2) and infrared (IR) spectra clearly confirmed that there were almost no trapped, remaining BDC-NH2Cl and DABCO ligands after washing process of DMOFs (by DMF and chloroform, Figures S3-S5). Thermogravimetric analysis (TGA) showed that all six regioisomeric DMOFs with different metal salts offered good thermal stability. Generally, DMOF(Cu)s showed decomposition temperatures >250 °C, and

DMOF(Co)s/DMOF(Zn)s are thermally stable up to 300 °C (Figure S6). Around 36-55 weight% losses were observed by ligand portion before 500 °C (Figure S7-S9).

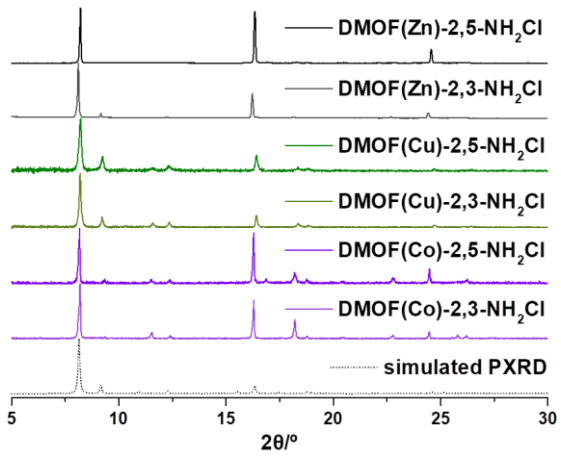

Figure 1. PXRD patterns of regioisomeric DMOFs with different metals.

N_2 Adsorption Experiments of Regioisomeric DMOFs

The N_2 adsorption differences among six different regioisomeric DMOFs after evacuation were studied at 77 K (Figures 2 and S10). In previous studies, flexibility changes upon evacuation were observed by comparing the amounts of N_2 adsorbed with NH_2-Cl, NH_2-Br, NH_2-OMe and OMe-OMe substituents at different positions. In other words, DMOF(Zn)-2,5-NH_2Cl, which has narrow pores after evacuation, is almost nonporous to N_2, meaning that it has a flexible-irreversible structure. However, DMOF(Zn)-2,3-NH_2Cl, which is not collapsed after evacuation, shows high N_2 uptake, indicating the structure is inflexible to evacuation. The N_2 uptake difference is approximately 350 m^2/g.[11] Once again, the as-synthesized DMOF(Zn)-2,3-NH_2Cl and DMOF(Zn)-2,5-NH_2Cl have almost identical structures (i.e., very similar PXRD patterns). Interestingly, in the case of cobalt-based DMOFs, there are no significant differences in the N_2 uptakes of DMOF(Co)-2,3-NH_2Cl and DMOF(Co)-2,5-NH_2Cl (Figure 2 and Table 1) upon evacuation. The difference in N_2 uptake is only <50 m^2/g. The type of isotherm and uptake amount follow patterns typical of DMOFs. This result strongly indicates that the flexibility of cobalt-based DMOFs was not altered by the regioisomer of the BDC-NH_2Cl ligand (**1** or **2**).

Table 1. N_2 uptake amount by DMOFs with regioisomeric ligands (at a relative pressure of $P/P_0 = 0.95$)

DMOF	DMOF(Co)	DMOF(Cu)	DMOF(Zn)[9]
BDC-2,3-NH_2Cl	354 cm^3/g	473 cm^3/g	363 cm^3/g
BDC-2,5-NH_2Cl	313 cm^3/g	306 cm^3/g	5 cm^3/g

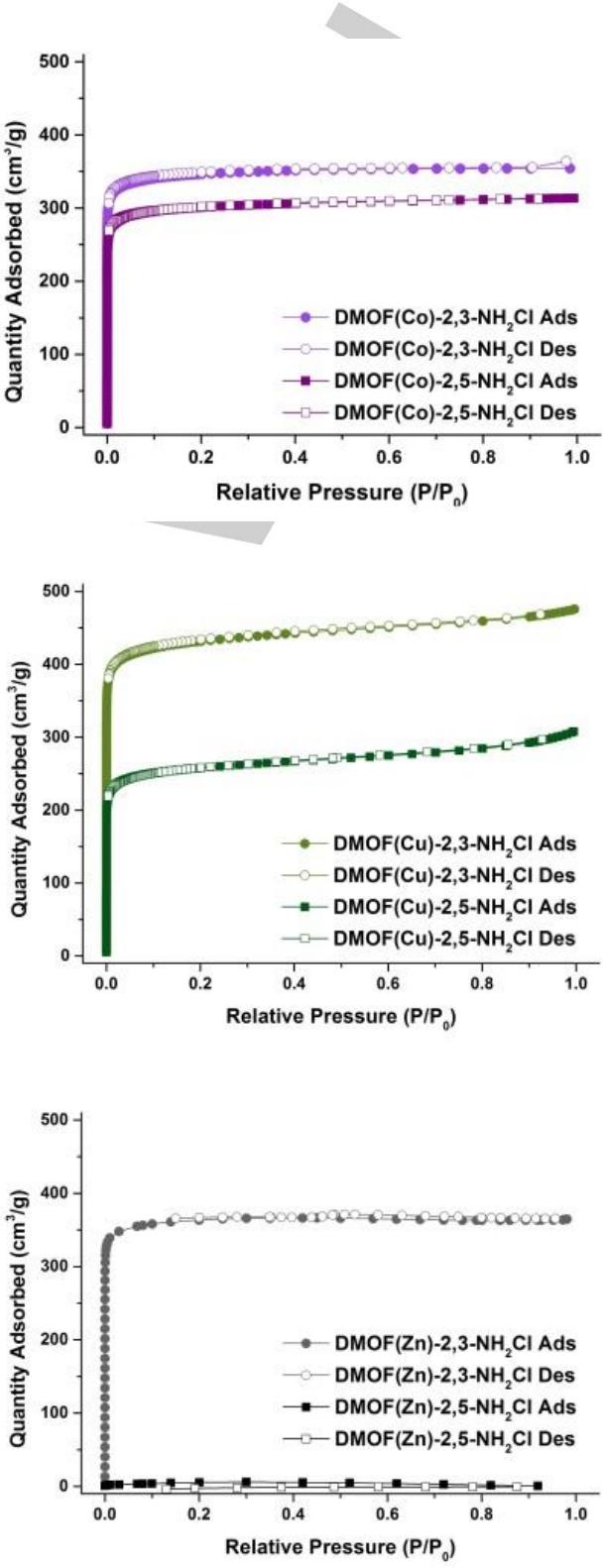

Figure 2. N_2 full isotherm at 77 K of regioisomeric DMOFs with different metals.

In the case of copper-based DMOFs, moderate differences in N_2 uptake between DMOF(Cu)-2,3-NH_2Cl and DMOF(Cu)-2,5-NH_2Cl were observed (~170 m^2/g). Nevertheless, DMOF(Cu)-2,3-NH_2Cl showed a regular DMOF-1 N_2 full isotherm pattern, meaning it is inflexible. The N_2 uptake by DMOF(Cu)-2,5-NH_2Cl is lower than that of DMOF(Cu)-2,3-NH_2Cl; however, this higher N_2 uptake was in contrast with the almost nonporous DMOF(Zn)-2,5-NH_2Cl. In 2015, Verpoort et al. reported four different highly porous DMOFs based on BDC-Ni, Co, Cu, and Zn. Their N_2 uptake amounts at saturation were approximately 400~500 cm^3/g.[24] Therefore, the low N_2 uptakes of DMOF(Cu)-2,5-NH_2Cl and DMOF(Zn)-2,5-NH_2Cl are caused by the functional groups and regioisomerism-derived flexibility-irreversibility upon evacuation before N_2 adsorption. Once again, these six regioisomeric DMOFs showed almost identical PXRD patterns in their as-synthesized states, and the differences in their N_2 uptake amounts varied between regioisomers.

Structural Analysis of the DMOFs

The functionalization studies provided experimental evidence of the relationship between electron density and the flexibility of the MOF. More electron-rich ligands could allow flexibility changes by regioisomerism (BDC-NH_2-X, BDC-NH_2-OMe, and BDC-$(OMe)_2$).[11–13] In the present study, we have the same functional groups on the ligands but different metals; thus, the coordination bonds between the SBUs and ligands should be carefully analyzed. The single-crystal structures of solvated DMOF(Zn)-2,3-NH_2Cl and DMOF(Zn)-2,5-NH_2Cl have been reported previously,[11] and the structure of solvated DMOF(Co)-2,5-NH_2Cl and desolvated (dried) DMOF(Zn)-2,3-NH_2Cl was solved for the first time in this work (Figures S11, S12 and Tables S1, S2). The diffraction data of DMOF(Co)-2,3-NH_2Cl was not suitable for determining its crystal structure. Unlike DMOF(Co)-2,3-NH_2Cl, DMOF(Zn)-2,5-NH_2Cl gives nice diffraction pattern, but it fails to determine the unit cell using the diffraction data. Despite good diffraction peaks in PXRD, it was impossible to even index the unit cell of the framework. The overall structures of DMOF(Co)-2,5-NH_2Cl (solvated), DMOF(Zn)-2,3-NH_2Cl (solvated), DMOF(Zn)-2,3-NH_2Cl (desolvated) and DMOF(Zn)-2,5-NH_2Cl (solvated) from their crystallographic data are consistent with the reported structures of DMOFs, as originally evidenced by their PXRD patterns (Figures 1, S11, and S12). Then, their single-crystal structures were carefully analyzed with a focus on the metal cluster geometries and bond lengths (Tables 2 and S3). First, we compared the metal-oxygen bond (M-O bond) distances (d_{M-O}) of the DMOFs. Interestingly, DMOF(Zn)-2,3-NH_2Cl has the shortest average M-O bond length, whereas the M-O bond lengths in DMOF(Co)-2,5-NH_2Cl and DMOF(Zn)-2,5-NH_2Cl are similar. The small difference between the M-O bond lengths of DMOF(Co)-2,5-NH_2Cl and DMOF(Zn)-2,5-NH_2Cl may be derived from the ionic radius of Co being smaller than that of Zn. The shorter bond length (0.042 Å, 2.1%) in DMOF(Zn)-2,3-NH_2Cl relative to those of DMOF(Co)-2,5-NH_2Cl and DMOF(Zn)-2,5-NH_2Cl suggests slightly stronger M-O bonding. In addition, the metal-nitrogen bond length in the DABCO pillar ligand of DMOF(Zn)-2,3-NH_2Cl was slightly longer than the M-N bond in DMOF(Zn)-2,5-NH_2Cl. However, the large N_2 adsorption differences between DMOF(Zn)-2,3-NH_2Cl/DMOF(Zn)-2,5-NH_2Cl and/or DMOF(Co)-2,5-NH_2Cl/DMOF(Zn)-2,5-NH_2Cl are not fully explained by the small structural differences in their solvated crystals. Moreover, the states of the samples are not matched since the N_2 adsorption experiments were conducted on activated (i.e., evacuated and fully dried) samples, and the crystal structures were obtained from the solvated species.

Table 2. M-O bond distances of DMOF(Co)-2,5-NH2Cl, DMOF(Zn)-2,3-NH2Cl, and DMOF(Zn)-2,5-NH2Cl in the solvated crystal structures

DMOFs	d (Å) (M-O1)	d (Å) (M-O2)	d (Å) (M-O3)	d (Å) (M-O4)	average d (Å) (M-O)
DMOF(Co)-2,5-NH_2Cl	2.0319	2.0216	2.0488	2.0552	2.0394
DMOF(Zn)-2,3-NH_2Cl (solvated)	1.9437	1.9437	2.0609	2.0609	2.0023
DMOF(Zn)-2,3-NH_2Cl (desolvated)	2.0190	2.0190	2.0190	2.0190	2.0190
DMOF(Zn)-2,5-NH_2Cl (solvated)	2.0364	2.0447	2.0671	2.0289	2.0443
DMOF(Zn)-2,3-NH_2Cl (desolvated)	Not determined	Not determined	Not determined	Not determined	Not determined

The flexible-irreversible structural changes in DMOF(Zn)-2,5-NH_2Cl, unlike the other DMOFs (DMOF(Co)s, DMOF(Cu)s, and DMOF(Zn)-2,3-NH_2Cl), were observed based on the PXRD pattern shift after evacuation (Figure S13). Other DMOFs showed no significant shifts in their PXRD data. Since the PXRD data could provide structural information, we attempted to collect PXRD data with better resolution and signal-to-noise ratio (Figures S14-S22). We tried to determine the unit cell parameters of the DMOFs (Table S4). The both DMOFs possessing cobalt ions have similar unit cell parameters (DMOF(Co)-2,3-NH_2Cl and DMOF(Co)-2,5-NH_2Cl), which supports their similar N_2 uptakes (Figures S14-S16). However, we found a significant increase in the background noise in the PXRD pattern for DMOF(Cu)-2,5-NH_2Cl, which suggests partial decomposition of the framework. Because of the partial decomposition, DMOF(Cu)-2,5-NH_2Cl has a smaller N_2 sorption amount compared to that of DMOF(Cu)-2,3-NH_2Cl (Figures S17-S19). The unit cell parameters of DMOF(Zn)-2,3-NH_2Cl were also determined, and they were similar to the values calculated by single-crystal structure analysis. When the PXRD patterns of DMOF(Zn)-2,3-NH_2Cl and DMOF(Zn)-2,5-NH_2Cl were compared (Figures S20-S22), we found that the major peaks

corresponding to the (n,0,0) planes shifted to higher 2 theta values, which may be due to the shrinking of the framework (unit cell parameter reduction). In addition, many peaks in the PXRD pattern of DMOF(Zn)-2,5-NH_2Cl disappeared, but the peaks corresponding to the (n,0,0) planes did not. Although it is difficult to say that the structure of DMOF(Zn)-2,5-NH_2Cl was destroyed, it is clear that the DMOF(Zn) structures differ depending on the position of the functional groups on the BDC ligand. Because of the significant disappearances and decreases in diffraction peak intensity, it was impossible to determine the unit cell from the PXRD unit cell indexing process of DMOF(Zn)-2,5-NH_2Cl. We can estimate the unit cell parameters from the peak position of the MOFs and DMOF(Zn)-2,5-NH_2Cl has much smaller 2theta values in PXRD compared to that of DMOF(Zn)-2,3-NH_2Cl, which means the smaller unit cell parameter of the framework. In addition, peak intensities of the framework have been drastically changed, which also indicate local structure change in the framework. Although it was unable to determine the unit cell parameter of DMOF(Zn)-2,5-NH_2Cl, the significant difference of the PXRD pattern, implying an unusual change in the MOF structure.

Quantum Chemical Simulation Approaches

Next, we investigated the coordination environment differences of the simplified metal-ligand complexes using quantum chemical simulation approaches. Since the size of a MOF is nearly infinite, its structure is too large to be illustrated quantum chemically with current computational capabilities. Therefore, simplified model structures, M_2(BDC)(DABCO) complexes in which two divalent metal ions were held by four functionalized carboxylate ligands and capped with two DABCO units, were studied (*e.g.*, Co_2(BDC-2,3-$NH_2Cl)_4$(DABCO)$_2$/Co_2(BDC-2,5-$NH_2Cl)_4$(DABCO)$_2$, Cu_2(BDC-2,3-$NH_2Cl)_4$(DABCO)$_2$/Cu_2(BDC-2,5-$NH_2Cl)_4$(DABCO)$_2$, and Zn_2(BDC-2,3-$NH_2Cl)_4$(DABCO)$_2$/Zn_2(BDC-2,5-$NH_2Cl)_4$(DABCO)$_2$). The electronic mapping on the simplified repeating units is universal methodology on quantum chemical simulation approaches for polymeric material. The main interest of the current study is the flexibility upon evacuation, which is expected to strongly correlate with the structural environment around the metal dications. This model is expected to reproduce the original MOF's electronic and geometric features since it incorporates all the organic fragments directly bound to the metal dications. There are several possible conformers due to the relative orientation of the amine and chlorine substituents on the benzenes with respect to those on nearby benzenes. In this study, we focused on the statistically most likely combination–two amine groups (chlorine atoms) on the same side and the other two amine groups (chlorine atoms) on the opposite side. The minimum-energy structures were located by density functional theory (DFT) employing the ωB97X-D functional. The 6-31G* basis sets were used for the light atoms (hydrogen, carbon, oxygen, and chlorine), and LANL2DZ ECP and the corresponding basis sets were selected for describing the metal atoms. All quantum chemical simulations were performed with Q-Chem 5.1.[25]

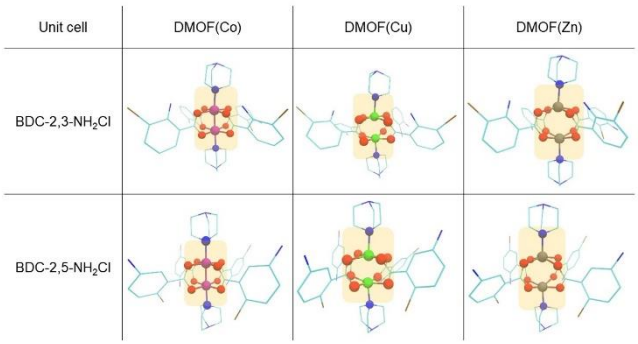

Figure 3. The predicted ground state structures of the model systems having Co, Cu, and Zn metal centers. The atoms directly connected to the metal ions are described with ball-and-stick models, and other atoms are described with simple line models. The hydrogen atoms have been omitted for clarity. Color scheme: carbon-cyan, nitrogen-blue, oxygen-red, chlorine-brown, cobalt-magenta, copper-green, and zinc-dark gray.

The ground state structures of the model systems having substituents at the 2,3- (*ortho*-, top) and 2,5-positions (*para*-, bottom) predicted by the quantum chemical simulations are displayed in Figure 3. (The top and side views are available in the Supporting Information, Figures S23-S25.) All six DMOF models in Figure 3 have five-coordinate metal centers, and their overall shapes are square pyramidal. Notably, the quantum chemical simulations located the minimum-energy structures of *four*-coordinate nickel ions (three oxygen atoms of carboxyl groups and one nitrogen of a DABCO) rather than five-coordinate metal centers like the others. This result provides one piece of evidence as to why we have not been able to synthesize DMOF(Ni)s (the optimized DMOF(Ni) structures are available in the Supporting Information, Figure S26). Inspired by the geometry index used in structural chemistry and crystallography,[26] we defined a new index (η) to quantify the regularity around the metal ions. This index measures the difference between the two largest oxygen-metal-oxygen angles ($\angle$OMOs, M: metal, and O: oxygen) in the highlighted region of Figure 3. There are two metal centers in the DMOF model; therefore, the numerical value of η is given as the average of two measurements. A zero value of η indicates that the structure around the metal atom is highly ordered regardless of its point group symmetry. In other words, both perfect square pyramidal geometries (i.e., the two $\angle$OMOs are the same, and the values are 180°) and distorted square pyramidal geometries (the two $\angle$OMOs are the same but are <180°) could have η values equal to 0. A large η value means that the two $\angle$OMOs are significantly different. Therefore, the structures around the metal center are less ordered and are less sensitive to subtle geometric changes. This results in a number of different feasible local minimum structures; therefore, compounds with low symmetry would be more flexible than highly symmetric compounds.

Table 3 lists the numerical values of $\angle$OMO of the six DMOF models studied herein. The DMOF structures with cobalt as the

central metal atoms are nearly perfect square pyramids, and the two ∠OMO values are nearly the same (approximately 180°) regardless of the positions of the substitutions. The DMOF(Cu)s feature more distorted square pyramidal geometries than are found in the cobalt derivatives. The largest deviation from square pyramidal geometry was observed for the DMOF(Zn)s. The values of ∠OMO were significantly lower (150~160°). While DMOF(Zn)-2,3-NH_2Cl is well-ordered (i.e., the two ∠OMOs are nearly the same, and they give an η value of only 0.5), the coordination environment of DMOF(Zn)-2,5-NH_2Cl is quite asymmetric. Generally, DMOF(M)-2,3-NH_2Cl yields structures that are relatively more symmetric and ordered than those of DMOF(M)-2,5-NH_2Cl, which could explain the observed rigidity (inflexibility) of DMOF(M)-2,3-NH_2Cl (M = Co, Cu, and Zn). Within the DMOF(M)-2,5-NH_2Cl series, the η values become larger as the metal atoms are varied from Co to Zn. As a small η value implies a well-ordered structure, these results explain the inflexibility of DMOF(Co)-2,5-NH_2Cl, lower flexibility of DMOF(Cu)-2,5-NH_2Cl, and flexibility of DMOF(Zn)-2,5-NH_2Cl upon evacuation. We found that the trend in the O-M-O angles does not exactly match the X-ray crystallographic data of solvated DMOF(Co)-2,5-NH_2Cl, DMOF(Zn)-2,3-NH_2Cl, and DMOF(Zn)-2,5-NH_2Cl (Table 2 and Table 3). The discrepancy may be derived from the difference of the solvent system and the unit-framework.

Table 3. Numerical values of ∠OMO (°) and index η (°) for DMOF(M)-2,3-NH_2Cl and DMOF(M)-2,5-NH_2Cl. (M=Co, Cu, and Zn)

MOFs	Parameters	Co	Cu	Zn
DMOF(M)-2,3-NH_2Cl	1st metal center ∠OMO (°)	176.5	173.8	157.0
		176.0	164.1	156.1
	2nd metal center ∠OMO (°)	176.6	171.2	153.7
		175.8	163.2	153.6
	η	0.6	8.9	0.5
DMOF(M)-2,5-NH_2Cl	1st metal center ∠OMO (°)	176.8	171.5	160.9
		176.1	164.0	150.0
	2nd metal center ∠OMO (°)	175.7	174.2	160.6
		175.5	163.5	149.6
	η	0.5	9.1	11.0

Conclusions

Four new, bifunctional (NH_2-Cl) DMOFs have been successfully synthesized using cobalt and copper salts. A total of six series of DMOFs (including two previously reported Zn-DMOFs) were compared to study the effect of the metal on the magnitude of the changes in flexibility with two regioisomeric ligands (BDC-2,3-NH_2Cl and BDC-2,5-NH_2Cl). Although regioisomeric functionalized DMOFs with nickel salts were not obtained, we could clearly observe the trends and relationships between the metal salts and changes in flexibility. All six regioisomeric DMOFs have similar frameworks their as-synthesized forms, as evidenced by their PXRD patterns; however, different regioisomers of the ligands resulted in different magnitudes of changes in their N_2 uptakes. In particular, the N_2 uptake differences are very small in cobalt-based DMOFs, moderate in copper-based DMOFs, and large in zinc-based DMOFs. Although all DMOF(M)-2,3-NH_2Cl derivatives showed high porosity after evacuation and followed the typical N_2 full isotherm of DMOFs at 77K, DMOF(M)-2,5-NH_2Cl derivatives displayed very different N_2 uptake behaviors. High porosity for DMOF(Co)-2,5-NH_2Cl, moderate porosity for DMOF(Cu)-2,5-NH_2Cl, and poor porosity for DMOF(Zn)-2,5-NH_2Cl after evacuation were observed. This result means that DMOF(Zn)-2,5-NH_2Cl has a flexible-irreversible structure upon evacuation, but the N_2 uptake of DMOF(Cu)-2,5-NH_2Cl is reduced, and DMOF(Co)-2,5-NH_2Cl is inflexible. All three DMOF(M)-2,3-NH_2Cl species were, of course, inflexible upon evacuation (M = Co, Cu, and Zn).

While the PXRD patterns of all six as-synthesized DMOFs matched and there were no significant differences in the X-ray crystallographic data of solvated DMOF(Co)-2,5-NH_2Cl, DMOF(Zn)-2,3-NH_2Cl, and DMOF(Zn)-2,5-NH_2Cl, only DMOF(Zn)-2,5-NH_2Cl (i.e., flexible-irreversible structures) showed significant changes in their PXRD patterns after evacuation. In addition, quantum chemical simulation approaches helped clarify our findings. A new index (η) was defined to quantify the regularity of the structural environment around the metal ion based on differences in the oxygen-metal-oxygen bond angles (∠OMOs). Within the BDC-2,5-NH_2Cl series, the η value becomes larger as the metal atoms are varied from Co to Zn. As a small η value implies a well-ordered structure, these results justify the inflexibility of DMOF(Co)-2,5-NH_2Cl, the limited flexibility of DMOF(Cu)-2,5-NH_2Cl, and the flexibility of DMOF(Zn)-2,5-NH_2Cl upon evacuation. Finally, in the case of DMOF(Ni)s, the nickel unit cells with BDC-2,3-NH_2Cl and BDC-2,5-NH_2Cl were not formed in the quantum chemical simulation because the minimum energy was identified with a four-coordinate nickel species. This result is consistent with our experimental results; our thorough testing of synthetic conditions for DMOF(Ni)-2,3/2,5-NH_2Cl were not successful. This study suggests that the metal cation, coordination environment of the metal-ligand, and the position of functional groups in ligand are important for MOF synthesis and the resulting properties, including flexibility.

Experimental Section

DMOF(Co)-2,3-NH_2Cl: BDC-2,3-NH_2Cl (**1**, 107 mg, 0.5 mmol) and $Co(NO_3)_2{\cdot}6H_2O$ (146 mg, 0.5 mmol) were dissolved in 12.5 mL of DMF. The pillar ligand (DABCO, 56 mg, 0.5 mmol) was added to this mixture. A purple gel formed upon the addition of DABCO. The gel was filtered through a fritted disc of fine porosity. The solution was then transferred to an autoclave and heated at a rate of 2.5 °C/min from room temperature

to 120 °C. The temperature was then held for 48 h, and the material was cooled to room temperature at a rate of 2.5 °C/min. The resulting crystals were then washed three times with 5 mL of DMF. The solvent was then exchanged with chloroform (5 mL) over three days, replacing the old chloroform with fresh chloroform every 24 h.

DMOF(Co)-2,5-NH_2Cl: BDC-2,5-NH_2Cl (**2**, 107 mg, 0.5 mmol) was used instead of BDC-2,3-NH_2Cl (**1**) with the same protocol as was used for the synthesis of DMOF(Co)-2,3-NH_2Cl.

DMOF(Cu)-2,3-NH_2Cl: BDC-2,3-NH_2Cl (**1**, 107 mg, 0.5 mmol) and $Cu(NO_3)_2{\cdot}3H_2O$ (121 mg, 0.5 mmol) were dissolved in 12.5 mL of DMF. The pillar ligand (DABCO, 56 mg, 0.5 mmol) was added to this mixture. A green gel formed upon the addition of DABCO. The mixture was then transferred to a scintillation vial and heated at a rate of 2.5 °C/min from room temperature to 120 °C. The temperature was then held for 24 h, and then the material was cooled to room temperature at a rate of 2.5 °C/min. The resulting crystals were then washed three times with 5 mL of DMF. The solvent was then exchanged with chloroform (5 mL) over three days, replacing the old chloroform with fresh chloroform every 24 h.

DMOF(Cu)-2,5-NH_2Cl: BDC-2,5-NH_2Cl (**2**, 107 mg, 0.5 mmol) was used instead of BDC-2,3-NH_2Cl (**1**) with the same protocol as was used for the synthesis of DMOF(Cu)-2,3-NH_2Cl.

X-ray Crystal Structure Analysis: A single crystal of the MOF was coated with Paratone-N oil, and the diffraction data were measured by synchrotron radiation (λ = 0.69999 Å) on an ADSC Quantum-210 detector at 2D SMC with a silicon (111) double-crystal monochromator (DCM) at the Pohang Accelerator Laboratory (PAL; Pohang, Korea). ADSC Q210 ADX software[27] was used for data collection (detector distance of 63 mm, omega scan; $\Delta\omega$ = 1°, exposure time of 10 s per frame), and HKL3000sm (Ver. 703r)[28] was used for cell refinement, reduction, and absorption corrections. The crystal structure was solved by the direct method using SHLEXT (2014/4)[28] for MOFs and refined by full-matrix least-squares refinement using the SHELXL (2014/7) computer program. For all the crystals, the contributions from disordered solvent molecules were removed by using the SQUEEZE routine (PLATON),[29] and the outputs from the SQUEEZE calculations are attached to each CIF file. The positions of all non-H atoms were refined with anisotropic displacement factors. All H atoms were placed using a riding model, and their positions were constrained relative to their parent atoms using the appropriate HFIX command in SHELXL-2014. The X-ray diffraction data for the MOFs were collected using synchrotron (PAL). The supplementary crystallographic data for this study are found in the CCDC-1909253 and CCDC-1919446 for DMOF(Co)-2,5-NH_2Cl and DMOF(Zn)-2,3-NH_2Cl, respectively. The data can be obtained free of charge from www.ccdc.cam.ac.uk/conts/retrieving.html (or from the CCDC, 12 Union Road, Cambridge CB2 1EZ, UK; fax: +44 1223 336033; e-mail: deposit@ccdc.cam.ac.uk).

Acknowledgements

This research was supported by the Basic Science Research Program (2019R1A2C4070584) and the Science Research Center (2016R1A5A1009405) through the National Research Foundation of Korea (NRF) funded by the Ministry of Science and ICT.

Keywords: metal-organic frameworks • coordination polymers • metal cation effect • flexibility • regioselectivity

[1] H.-C. Zhou, J. R. Long, O. M. Yaghi, *Chem. Rev.* **2012**, *112*, 673–674.

[2] L. J. Murray, M. Dincă, J. R. Long, *Chem. Soc. Rev.* **2009**, *38*, 1294–1314.

[3] J.-R. Li, R. J. Kuppler, H.-C. Zhou, *Chem. Soc. Rev.* **2009**, *38*, 1477–1504.

[4] J. Lee, O. K. Farha, J. Roberts, K. A. Scheidt, S. T. Nguyen, J. T. Hupp, *Chem. Soc. Rev.* **2009**, *38*, 1450–1459.

[5] A. Schneemann, V. Bon, I. Schwedler, I. Senkovska, S. Kaskel, R. A. Fischer, *Chem. Soc. Rev.* **2014**, *43*, 6062–6096.

[6] A. Clearfield, *Dalton Trans.* **2016**, *45*, 4100–4112.

[7] T. Loiseau, C. Volkringer, M. Haouas, F. Taulelle, G. Férey, *C. R. Chim.* **2015**, *18*, 1350–1369.

[8] G. Férey, C. Serre, *Chem. Soc. Rev.* **2009**, *38*, 1380–1399.

[9] S. Henke, D. C. Florian Wieland, M. Meilikhov, M. Paulus, C. Sternemann, K. Yusenko, R. A. Fischer, *CrystEngComm* **2011**, *13*, 6399–6404.

[10] S. Henke, A. Schneemann, A. Wütscher, R. A. Fischer, *J. Am. Chem. Soc.* **2012**, *134*, 9464–9474.

[11] M. Kim, J. A. Boissonnault, P. V. Dau, S. M. Cohen, *Angew. Chem. Int. Ed.* **2011**, *50*, 12193–12196.

[12] H. Hahm, K. Yoo, H. Ha, M. Kim, *Inorg. Chem.* **2016**, *55*, 7576–7581.

[13] H. Ha, H. Hahm, D. G. Jwa, K. Yoo, M. H. Park, M. Yoon, Y. Kim, M. Kim, *CrystEngComm* **2017**, *19*, 5361–5368.

[14] N. Klein, H. C. Hoffmann, A. Cadiau, J. Getzschmann, M. R. Lohe, S. Paasch, T. Heydenreich, K. Adil, I. Senkovska, E. Brunner, et al., *J. Mater. Chem.* **2012**, *22*, 10303–10312.

[15] F. Nouar, T. Devic, H. Chevreau, N. Guillou, E. Gibson, G. Clet, M. Daturi, A. Vimont, J. M. Grenèche, M. I. Breeze, et al., *Chem. Commun.* **2012**, *48*, 10237–10239.

[16] J. Bergmann, K. Stein, M. Kobalz, M. Handke, M. Lange, J. Möllmer, F. Heinke, O. Oeckler, R. Gläser, R. Staudt, et al., *Microporous Mesoporous Mater.* **2015**, *216*, 56–63.

[17] K. Kobalz, M. Kobalz, J. Möllmer, U. Junghans, M. Lange, J. Bergmann, S. Dietrich, M. Wecks, R. Gläser, H. Krautscheid, *Inorg. Chem.* **2016**, *55*, 6938–6948.

[18] Y.-C. Ou, Y.-Y. Song, M.-M. Hao, J.-Z. Wu, J.-Z. Wu, Y.-C. Ou, Y.-Y. Song, H.-M. Du, M.-M. Hao, J.-Z. Wu, *Crystals* **2017**, *7*, 311.

[19] A. Schneemann, P. Vervoorts, I. Hante, M. Tu, S. Wannapaiboon, C. Sternemann, M. Paulus, D. C. F. Wieland, S. Henke, R. A. Fischer, *Chem. Mater.* **2018**, *30*, 1667–1676.

[20] D. N. Dybtsev, H. Chun, K. Kim, *Angew. Chem. Int. Ed.* **2004**, *43*, 5033–5036.

[21] H. Jasuja, Y. Jiao, N. C. Burtch, Y. Huang, K. S. Walton, *Langmuir* **2014**, *30*, 14300–14307.

[22] D. Sarma, K. V. Ramanujachary, S. E. Lofland, T. Magdaleno, S. Natarajan, *Inorg. Chem.* **2009**, *48*, 11660–11676.

[23] R. Vismara, G. Tuci, N. Mosca, K. V. Domasevitch, C. Di Nicola, C. Pettinari, G. Giambastiani, S. Galli, A. Rossin, *Inorg. Chem. Front.* **2019**, *6*, 533–545.

[24] S. Chaemchuen, K. Zhou, N. A. Kabir, Y. Chen, X. Ke, G. Van Tendeloo, F. Verpoort, *Microporous Mesoporous Mater.* **2015**, *201*, 277–285.

[25] Y. Shao, Z. Gan, E. Epifanovsky, A. T. B. Gilbert, M. Wormit, J. Kussmann, A. W. Lange, A. Behn, J. Deng, X. Feng, et al., *Mol. Phys.* **2015**, *113*, 184–215.

[26] A. W. Addison, T. N. Rao, J. Reedijk, J. van Rijn, G. C. Verschoor, *J. Chem. Soc., Dalton Trans.* **1984**, *0*, 1349–1356.

[27] Z. Otwinowski, W. Minor, *Methods Enzymol.* **1997**, *276*, 307–326.

[28] G. M. Sheldrick, IUCr, *Acta Crystallogr. Sect. A Found. Crystallogr.* **2008**, *64*, 112–122.

[29] A. L. Spek, *Acta Crystallogr. Sect. C Struct. Chem.* **2015**, *71*, 9–18.

10.1002/chem.201903210

WILEY-VCH

Entry for the Table of Contents

FULL PAPER

The effect of metal on the degree of flexibility upon evacuation of paddle-wheel-type metal-organic frameworks (MOFs) has been revealed with positional control of the organic functionalities. The difference in the amount of N_2 taken by species with *ortho*- and *para*-substituents increased in the order of cobalt, copper, and zinc.

Hyeonbin Ha, Youngik Kim, Dopil Kim, Jihyun Lee, Yoodae Song, Suyeon Kim, Myung Hwan Park, Youngjo Kim, Hyungjun Kim, Minyoung Yoon*, Min Kim**

Page No. – Page No.

Effect of the metal within regioisomeric paddle-wheel type metal-organic frameworks